IJNRD.ORG ISSN : 2456-4184
INTERNATIONAL JOURNAL OF NOVEL RESEARCH AND DEVELOPMENT (IJNRD) | IJNRD.ORG
An International Open Access, Peer-reviewed, Refereed Journal

Optimum Slope Angle Determination with FLAC 2D And Q-Slope Methods at Oroutumba Sodalite Quarries in Namibia

Matheus Vaino Ipinge[1], Victor Mutambo[2],

[1,2] Department of Mining Engineering, School of Mines, University of Zambia

Abstract

Sodalite is one of the typical stones used in tombstone and tile manufacturing. Namibia's mining industry is vital in supplying the dimension stone if these sodalite rocks are mined in big blocks. However, the current surface mining method employed results in the extraction of smaller blocks of about 3 cm to 45 cm due to the application of improper slope angles and use of primitive extraction tools. The study was conducted at two (2) shallow pits operated by artisanal and small-scale (ASM) miners, mining a sodalite vein in a gabbro rock formation. The study evaluated the geomechanical parameters of the rock mass through application of the Finite Differential Method (FDM) and FLAC 2D software to establish the Safety of Factor (SOF) and optimum slope angle for sodalite mining up to a depth of 120 m. The optimum overall slope angle for both pits (Oroutumba pit 02 and Oroutumba 03) is 75°while the optimum pit depths were found to be 120 m and 80 m respectively.

Keywords: Slope angle; Finite deferential method; FLAC 2D, Safety of Factor, sodalite mining

1. Introduction

Most sodalite quarries in Namibia are located in the northern part of Kunene region[1][2][3]. The region is arid and receives an annual mean rainfall of about 200 mm[4]. Artisanal and small-scale miners (ASMs) are the major players in the sodalite mining industry[5][6]. However, the ASMs lack funds and mining technical skills and employ primitive tools[7][8][9][10][11]. Another drawback is that they primarily mine sodalite in small blocks ranging from 3 cm to 45 cm[11]. The size of the blocks makes it difficult to supply to lucrative international markets[5] and often times ended up with the tourists being the only customers [10].

The study was conducted at 2 shallow sodalite pits (Fig.1 and 2) located in the Oroutumba area.

Fig 1: Oroutumba pit 03

Fig 2: Oroutumba pit 02

Oroutumba pit 02 (-17.340936°, 13.786071°) in Fig 1 and Oroutumba pit 03 (-17.339248°, 13.783323°) in Fig 2, both operating pits with depths ranging from 3m to 5 m, about 4 m in width and the slope angle ranging from 45° to 90°, these pits are characterised by gabbro rocks and sodalite bearing dike[12] which formed as a result of carbonatite intrusion[13][14][15][16]. Information from 3 boreholes indicated that the water table lies about 120 to 150 m[16]. The study aims to evaluate the geomechanical parameters of the rock mass through finite differential and empiric methods to establish the overall optimum slope angle for sodalite mining up to a depth of 120 m.

2. Material and methods

The slope hazard assessment was undertaken based on the empirical method Q-slope developed by Barton and the Finite Difference Method (FDM) with the application of FLAC 2D by calculating the factor of safety (FOS) [13]. FDM has been used to simulate the open pit high wall up to a depth of 120 m.

A. Determination of maximum stable Slope angle with Q-slope

1. RQD

RDQ is a standard technique in the Geotechnical, Geology and whole mineral industry for assessing rock quality, looking at the degree of joints, fracturing and shearing in the rock mass[17]. It is mainly used to evaluate rock mass from the core samples; however, this study assessed rock mass from the exposed lateral wall measuring the block larger than 100 mm[18].

$$RQD(\%) = \frac{\Sigma Length\ of\ rock\ blocks > 100\ mm}{Total\ length\ of\ the\ measured\ rock\ blocks} \times 100\% \qquad \text{(Equation 1)}$$

2. Determination of Jn, Jr, Ja, J wice and SRF

Comprehensive fieldwork was done, and then all the necessary geological information such as Joint number set ($J_{n)}$, Joint roughness (J_r), Joint alteration (J_r), environmental and geological factors influence (J_{wice}) and strength reduction factor (SRF) were recorded and evaluated based on Tables 1, 2, 3, 4, 5, 6, 7 and 8 to convert the ground condition into quantitative values for the calculation of Q-slope and Slope angle [19].

Table 1: Barton (2018) Rock quality Designation

RQD	**Description**	**RQD (%) ***
A	Very poor	0 – 25
B	Poor	25 – 50
C	Fair	50 – 75
D	Good	75 – 90
E	Excellent	90 – 100

Table 2: Barton (2018) Joint Set Number

Joint Set Number	**Description**	J_n
A	Massive, no or few joints	0,5 – 1
B	One joint set	2
C	One joint set plus a random joint	3
D	Two joint sets	4
E	Two joint sets plus random joints	6
F	Three joint sets	9
G	Three joint sets plus random joints	12
H	Four or more joint sets, random, heavily jointed	15
J	Crushed rock, earth-like	20

Table 3: Barton (2018) Joint Roughness Number

Joint Set Number	**Description**	J_n
A	Discontinuous joints	4
B	Rough or irregular, undulating	3
C	Smooth, undulating	2
D	Slickensides, undulating	1.5
E	Rough or irregular, planar	1.5
F	Smooth, planar	1
G	Slickensides, planar	0,5
H	A zone containing clay minerals thick enough to prevent rock wall contact.	1

J	Sandy, gravely or crushed zone thick enough to prevent rock wall contact.	1

Table 4: Barton (2018) Joint Roughness Number

Joint Alteration Number	**Description**	J_a
A	Tightly healed, hard, non-softening, impermeable fillings	0.75
B	Unaltered joint walls, surface staining only	1
C	Slightly altered joint wails	2
D	Silty or sandy clay coatings, small clay disintegrated rock	3
E	Softening or low-friction clay mineral coating	4
F	Sandy particle, clay-free disintegrated rock	4
G	Strongly over consolidated non-softening clay mineral fillings	6
H	Medium or low over-consolidation, softening, clay mineral fillings	8
J	Swellings clay fillings	8 - 12
M	Zone or bands of silty or sandy clay, small clay fraction.	6, 8
N	Thick, continuous zones or bands of clay	5

Table 5: Barton (2018) Environmental and Geological Condition Number

J_{wice} *	**Desert Environment**	**Wet Environment**	**Tropical storms**	**Ice Wedging**
Stable structure, competent rock	1	0.7	0.5	0.9
Stable structure, incompetent rock	0.7	0.6	0.3	0.5
unstable structure, competent rock	0.8	0.5	0.1	0.3
Unstable structure, incompetent rock	0.5	0.3	0.05	0.2

Table 6: Barton (2018) Strength Reduction Factor Physical Condition (SRF_a)

	Description	SRF_a
A	Slight loosening due to surface location, disturbance from blasting or excavation.	2.5
B	Loose blocks, sign of tension cracks and joints shearing, susceptibility to weathering, severe disturbance from blasting	5
C	As B, but strong susceptibility to weathering	10
D	Slope is in advanced stage of erosion and loosening due to periodic erosion by water and/or ice wedging effects	15
E	Residual slope with significant transport of material down slope	20

Table 7: Barton (2018) Strength Reduction Factor Stress and strength (SRF_b)

	Description	σ_c/σ_1	SRF_b
F	Moderate stress strength range	50 – 200	2.5 – 1
G	High stress strength range	10 – 50	5 – 2.5
H	Localised intact rock failure	5 – 10	10 – 5
J	Crushing or plastic yield	2.5 – 5	15 – 10
K	Plastic flow of strain softened material	1 – 2.5	20 – 15

Table 8: Barton (2018) Strength Reduction Factor Major Discontinuity (SRF_c)

	Description	Favourable	Unfavourable	Very Unfavourable	Causing failure If unsupported
L	Major discontinuity with little or no clay	1	2	4	8
M	Major Discontinuity with RQD_{100}=0 due to clay and crushed rock	2	4	8	16
N	Major discontinuity with RQD_{300}=0 due to clay and crushed rock	4	8	12	24

3. Q-slope value

The Q-slope is a modified generation of the Q system to fit the slope condition, and it is given in Equation 2. It can be broken down into three (3) components: the first component is the block size, the Second is the Shear strength, and the last part is the external factors and stress[19].

$$Qslope = \frac{RQD}{J_n} \times \left(\frac{J_r}{J_a}\right)_0 \times \frac{J_{wice}}{SRF} \qquad \text{(Equation 2)}$$

4. Slope angle β

The steepest slope angle has been determined from equation 3, and then β will be used with the Q-slope value in the Q-slope stability chart presented in Fig 12 to evaluate if the angle is stable[19].

$$\beta = 20log10Qslope + 65° \qquad \text{(Equation 3)}$$

B. Calculating the factor of safety with the finite difference method (FDM)

The factor of safety calculation was done through the Fast Lagrangian Analysis of Continua (FLAC 2D) advanced Geotechnical modelling software used in mining and civil engineering for analysing, testing and designing engineering structures in soil, rock incorporating in groundwater [20].

1. Slope design parameters

The primary step is to create a drawing with the slope specifications, including design parameters: slope angle, slope height, slope depth and slope angle, as indicated in Fig 3. This drawing can be done in the FLAC 2D software or any other CAD software and then imported into the FLAC 2D software.

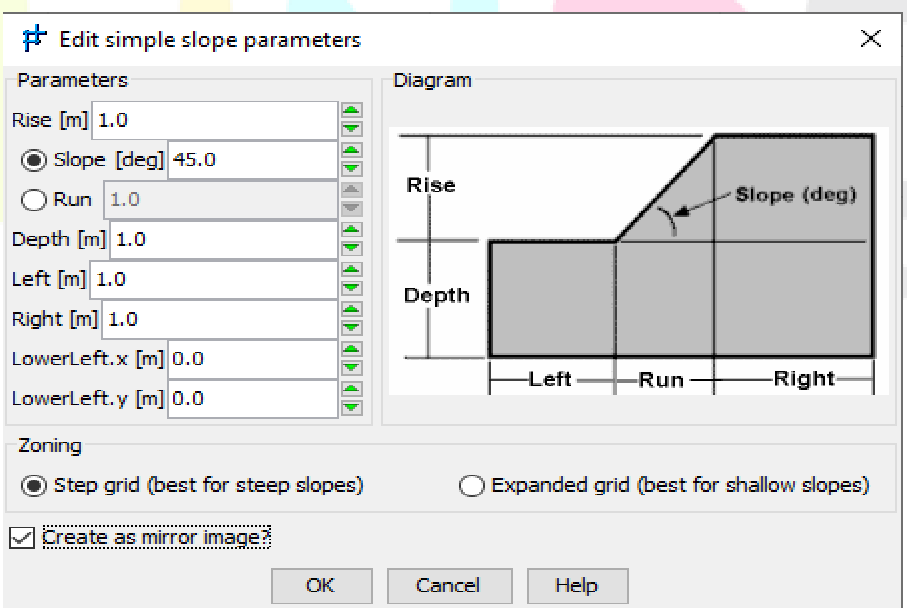

Fig 3: Interface of the simple slope design parameters

2. Geotechnical parameters

It is the critical stage where the boundary condition gets set to ground state (rollers in lateral and fixed at the bottom of the model), as indicated in Fig 4 of the model below.

Fig 4: Slope model boundary condition setting interface

Defining the finest mesh size of 100 was used in all models to minimise error even though it increased the duration of the model to run before converging. Fig 5 shows the interface of the mesh size selection.

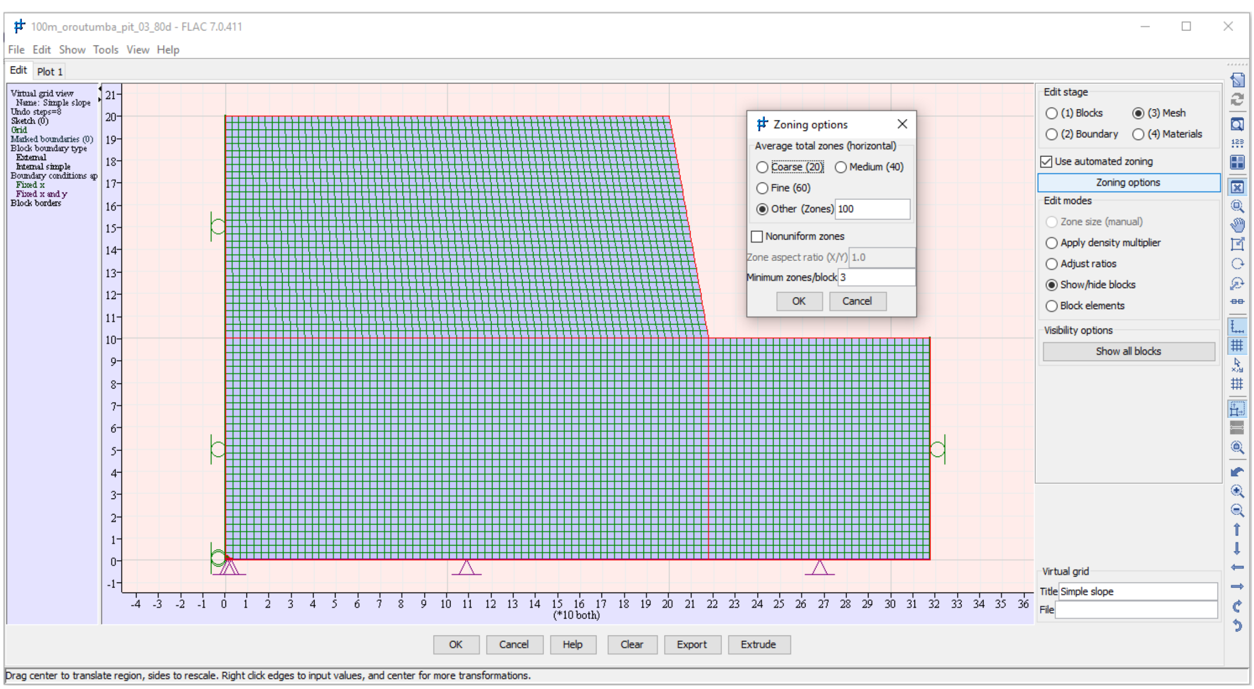

Fig 5: Mesh size setting interface

The final step is to define the rock stability model and material properties of the rock mass (presented in Table 2), as shown in Fig 6. All models were set to run the Hoek and Brown model, so stresses and strain were also considered during the FOS calculation [21][22][23].

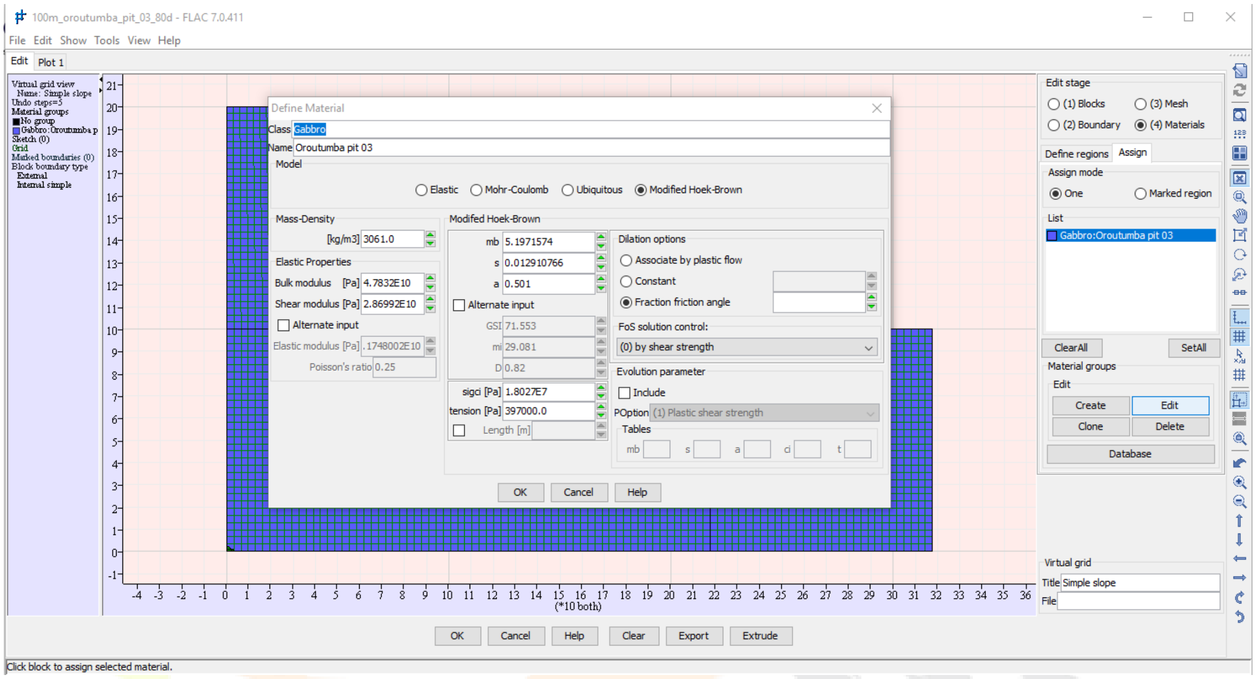

Fig 6: Rock stability model type and material properties setting interface

3. Other parameters

This step involves setting the gravitational force value at 9.81m/s^2, as shown in Fig 7.

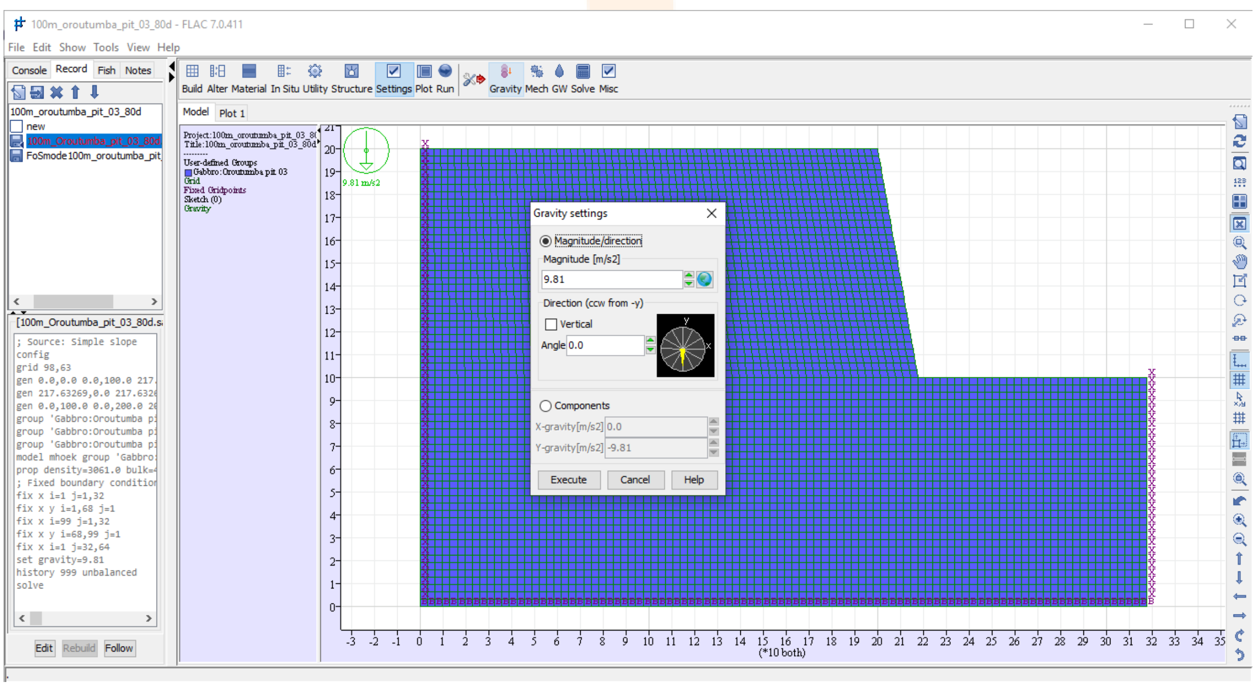

Fig 7: Gravitational force setting

Then, select the parameter to be displayed on the model outcome when it finishes the convergence process, as indicated in Fig 8.

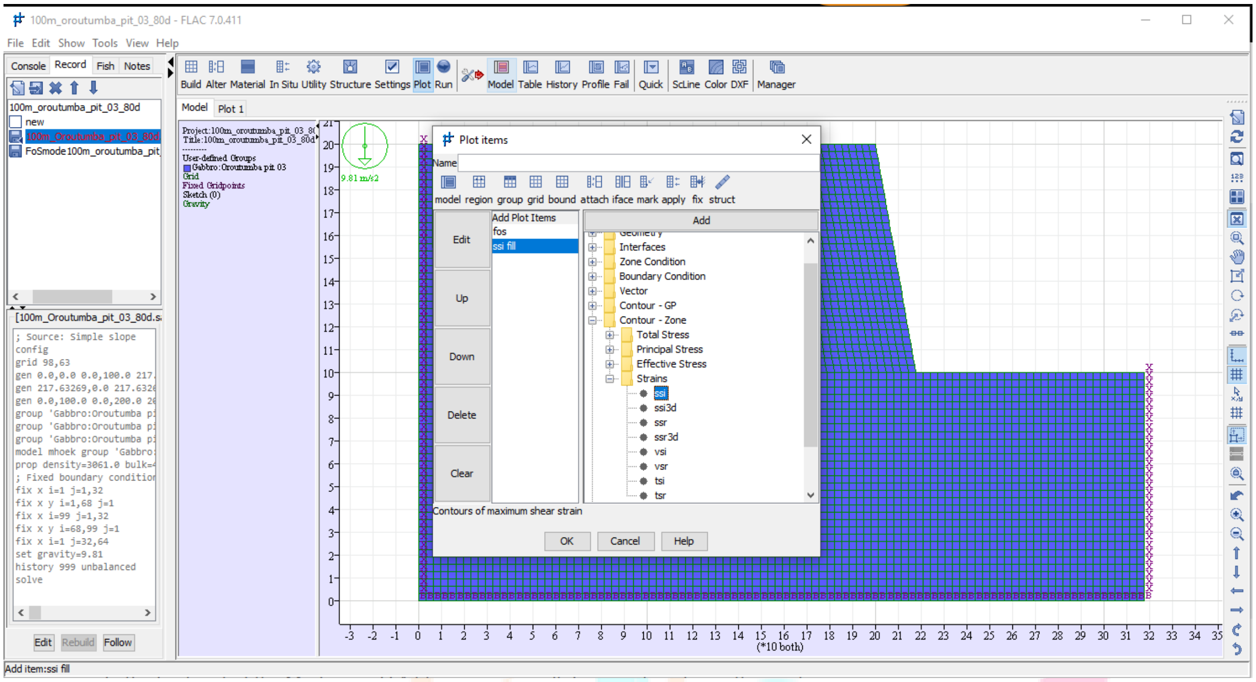

Fig 8: Interface of the outcome model displayed parameters

4. Calculation

FLAC 2D software uses the strength reduction method [24]. This method uses a reduction factor by dividing simultaneously the value of cohesion, friction angle, and intension parameters of the slope [14][25][26]. The new value obtained will be used as a new input parameter until the slope reaches the extreme state where the computing is not convergent [27][28][29]. The corresponding value will be the minimum safety factor of the slope [27][26][25]. The safety factor is assumed to be K=1 at the first iteration, then changes with computing, and C and φ are on the sliding plane[30].

$$C_e = \frac{C}{K} \qquad \text{(Equation 4)}$$

$$tan\emptyset_e = \frac{tan\emptyset}{K} \qquad \text{(Equation 5)}$$

the FLAC 2D iterate computation of stress-strain load with a boundary condition applied on the rock slope[31][21]. The components of the sliding surface are given by the resisting force F_r equation and driving force F_t in equation[28].

$$F_r = \frac{1}{t}\sum_{i=1}^{N_e} \sum_{g=1}^{N_g}(-tan\emptyset_{ei}\sigma_{nig} + C_{ei})V_{ig} \qquad \text{(Equation 6)}$$

$$F_t = \frac{1}{t}\sum_{i=1}^{N_e} \sum_{g=1}^{N_g}|\tau_{nig}|V_{ig} \qquad \text{(Equation 7)}$$

N_e is the total number of elements, N_g is Gauss integral in each element, σ_{nig} is the positive stress on Gauss point g in element i, τ_{rig} is the shearing strength on Gauss point g in element i, V_{ig} is the control volume, t is the thickness of the element i on sliding surface, φ_{ei} is the angle of friction reduction of element i, C_{ei} is cohesion reduction while $\sigma_{nig} \geq 0$, which is zero [25].

The equation gives the factor of safety

$$K^* = K \sum_{e=1}^{N_e} F_r / \sum_{e=1}^{N_e} F_t \quad \text{(Equation 8)}$$

This final step starts with solve and is followed by the model RUN command[28]. The model takes 4 to 6 hours to converge, and then the outcome models showing the FOS and shear strain rate are presented in Fig 9, Fig 10, Fig 11 and Fig 12.

3. Results

The slope evaluation includes the capability of the same rock mass to withstand its own weight, surcharge, and gravitational force without deformation and displacement [31]. The parameters such as Rock quality designation (RQD), the presence of water, the inclined plane toward the pit, faults and filling materials[26] negatively affect the rock stability. Therefore, there has always been a need to collect field data to determine/calculate the factor of safety for the rock slope stability analysis [32]. Table 9 summarises the slope stability parameter for two (2) pits.

Table 9: Summary of Q-slope analysis for Oroutumba sodalite pits

Summary of Qslope analysis Oroutumba sodalite quarries			
		Mine Name	
parameters		**Oroutumba Pit 03**	**Oroutumba pit 02**
RQD (%)	Mean	91.67	72.40600316
Jn	Mean	14.25	9
Jr	Mean	2	2
Ja	Mean	0.75	0.75
J wice	Mean	1	1
SRF	Mean	2.5	2.5
Qslope	Mean	6.9	8.581452226
β (°)	Mean	76.75	78.65

The results presented in Table 9 were assessed with an empiric rock stability method called Barton's (2018) slope analysis (Q-slope), similar to the Q system. Oroutumba pit 03 is a composition of fresh gabbro rock with a mean RQD value of 91.67%, which contains four joint sets which are heavily jointed. On a Barton, slope analysis scored the highest mean value (14.25). Its joint roughness is smooth, undulating, filled with the tightly healed, hard, non-softening, and impermeable filling of quartz. The rock structure is dry, stable, and competent enough to support engineering structures; it is worth noting that it does not present any evidence of harsh environmental conditions. It also possesses a high strength reduction value due to its high compression ratio against the load. Due to its competence, this Gabbro rock scored the Q-slope mean value (6.9), corresponding to the steep mean slope angle of 76.75°.

Oroutumba pit 02 is also made up of hard gabbro rock with three (3) joint sets and a mean RQD value of 72.4%. This rock mass has similar conditions of Joint roughness, joint alteration, environmental and geological conditions, and strength reduction factor. This rock formation scores the highest steep mean slope of 78.62°. The maximum stable slope angle on the Q-slope stability chart is 85°.

3.1 Factor of safety with FLAC 2D

The factor of safety (FOS) is a vital KPI used to measure the stability of the slope. The targeted value ranges from 1.0 to 1.30 depending on the competence of the rock and instability history [33]. All the factors of safety (FOS) for the study were determined with the application of modelling slopes in the FLAC 2D geotechnical tool, which uses the finite element under the strength reduction method, whereby it decreases the slope's strength parameters until the slope becomes unstable[31]. Then, the safety of the factor is given by the ratio between actual strength parameters and critical strength parameters [34]. The following geological and geotechnical information presented in Table 10 simulated the slope stability from 1.5m to 120 m.

Table 10 summarises the geological and geotechnical information for the rock mass of two (2) pits.

Name	**Oroutumba pit 02**	**Oroutumba pit 03**
Sample UCS (Mpa)	266.06	159.44
Rock type	Gabbro	Gabbro
GSI	70	70
Disturbance Factor	0.7	0.7
Rock mass intact modulus Ei (Mpa)	119728.04	71746.50
Rock mass cohesion (Mpa)	19.36	11.60
Rock mass Unit weight (ɣ) KN/m2	30035.96	28142.00
Rock mass friction angle (°)	40.17	40.17
Rock mass tensile (Mpa)	-0.66	-0.40
Rock mass UCS (Mpa)	30.08	18.03
Rock mass global strength	83.35	49.95
Rock mass deformation modulus	40421.96	24222.69
mb	5.194	5.194
s	0.0129	0.0129
a	0.501	0.501

Oroutumba pit 02

Fig 9 indicates the factor of safety of the pit at 3m and an angle of 75°, while Fig 10 shows the pit slope stability at 120 m with the same angle.

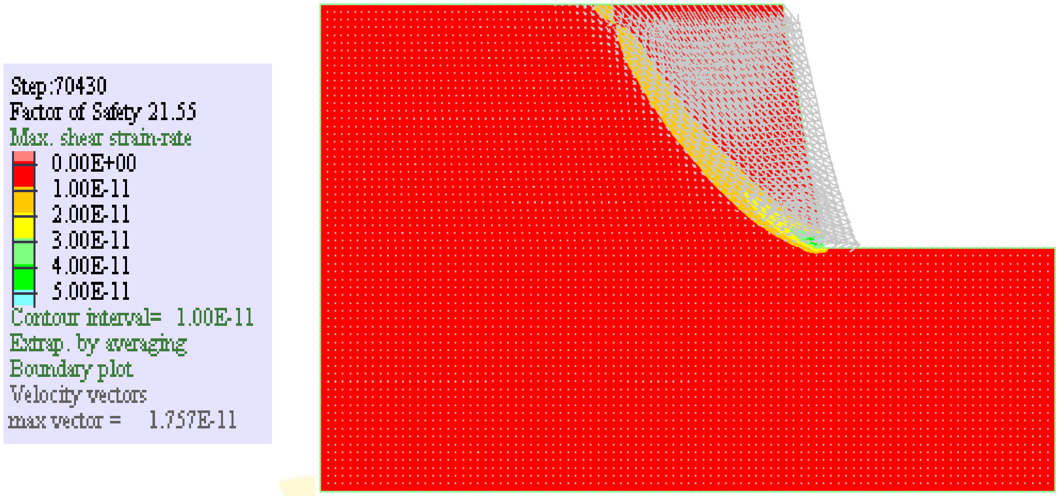

Fig 9: Oroutumba pit 02 Slope factor of safety at 3 m depth and angle of 75°

It is evident that the gabbro rocks have excellent quality rock strength. This rock mass is competent enough to support an engineering structure. The current mining operation is at a depth of 3m, a slope angle of 75° and a maximum shear strain rate of $5x10^{-11,}$ as indicated in Fig 9. At this level, the slope of the pit does not pose any chance of failure.

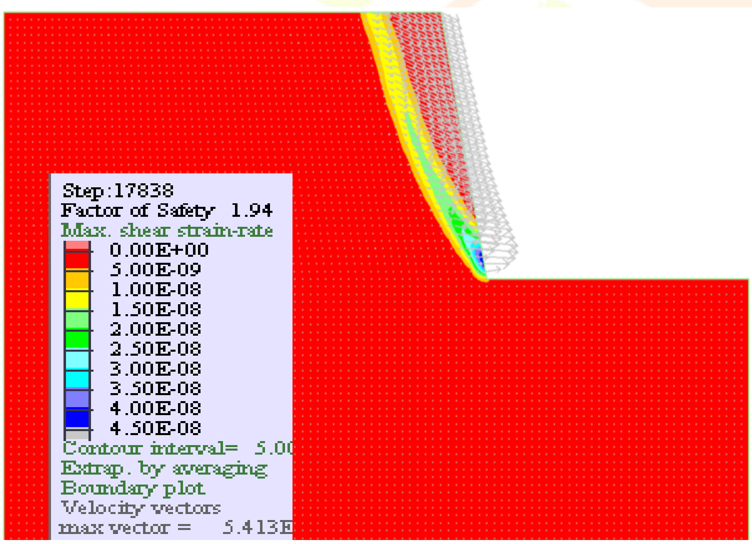

Fig 10: Oroutumba pit 02 Slope factor of safety at 120 m depth and angle of 75°

Fig 10 indicated that the maximum pit depth at 75°is up to 120 m with the maximum shear strain rate of 4.5×10^{-08}. This area is dry with a desert environment, with a lot of drilled boreholes with very little water at a depth of around 150m; since the water table (approximately from 100 to 120 m) could not be established, the safety is kept very high at 1.94 to account for water. In case of a slope failure, this could be a planar failure, and mining at this pit is profitable since the KPI strip ratio is minimal.

Oroutumba pit 03

Fig 11 and 12 also present the behaviour of the overall slope angle of the pit in the Gabbro rock formation to mine the sodalite. Rock failure is generally caused by the vertical and horizontal pressure trying to find equilibrium after a disturbance in the state of the said stresses. Fig 11 represents the current state of mining, and it can be seen that the factor of safety is relatively high at 21.55. with a maximum shear strain rate of about $5x10^{-09.}$ This strain is relatively minimal to cause shear along the failure plane since the rock mass poses a high friction force of 40.17.

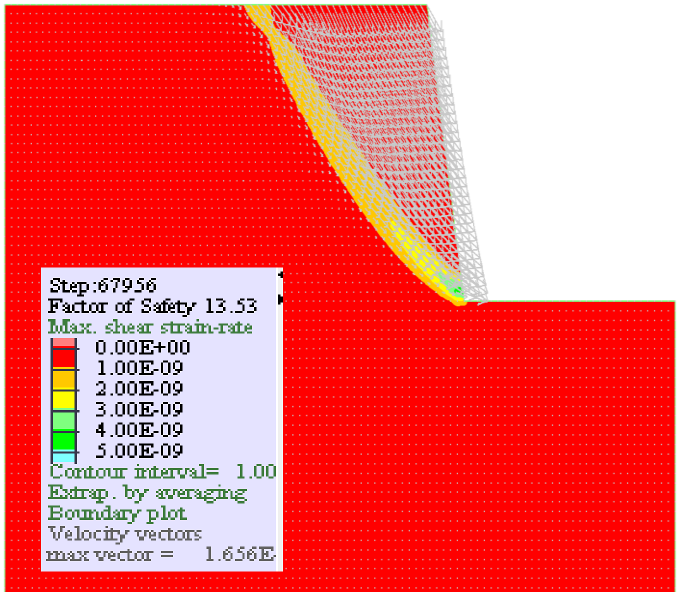

Fig 11: Oroutumba pit 03 Slope factor of safety at 3m depth and angle of 75°

The projected mining depth for this pit is 80m at the current angle of the slope, as indicated in Fig 12. The maximum shear strain rate the slope can handle without failing is $3.5 \times 10^{-07,}$ representing the factor of safety of 1.32. A wedge sliding failure could occur if the shear strain surpasses the limit.

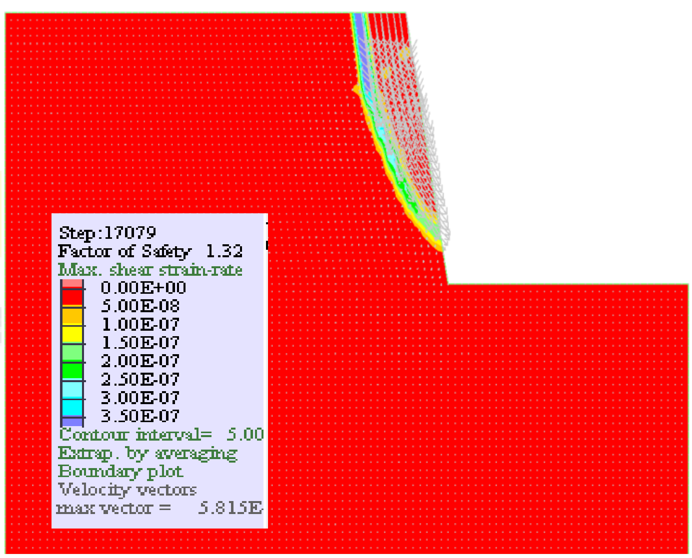

Fig 12: Oroutumba pit 03 Slope factor of safety at 80 m depth and angle of 75°

4. Discussion

The data suggest that fresh rocks are usually associated with high RQD and UCS. A low grade of discontinuity characterises high RQD and UCS rock mass [17]. Therefore, this media behaves more like an intact rock and can withstand a high wall with a steep angle compared to the rock mass with low values of RQD and UCS [35]. Oroutumba pit 02 has the most increased depth and steep slope angle, shown in Fig 9, while Oroutumba pit 03 can only reach a depth of 80 m with the same angle. The stable overall angle of the pits is less than the calculated angle presented in Table 1 and evaluated with the Qslope slope stability in Fig 13. The factor of safety used to simulate the slope angle is below the geotechnical FOS standard values presented in Table 11.

Table 11: slope stability FOS acceptable criteria values [Source: S. Peter et al. (2010)]

Slope scale	Consequences of failure	FOS
Bench	Low - High	1.1
Inter-ramp	Low	1.15 – 1.2
	Medium	1.2
	High	1.2 – 1.3
Overall	Low	1.2 – 1.3
	Medium	1.2 – 1.3
	High	1.3 – 1.5

All slope angle falls within the acceptable range of the FOS limit shown in Table 11. Moreover, the analysis conducted through Q-slope and finite difference method modelled with FLAC 2D suggest similar failure criteria and maximum stable slope angle of the gabbro formations[33].

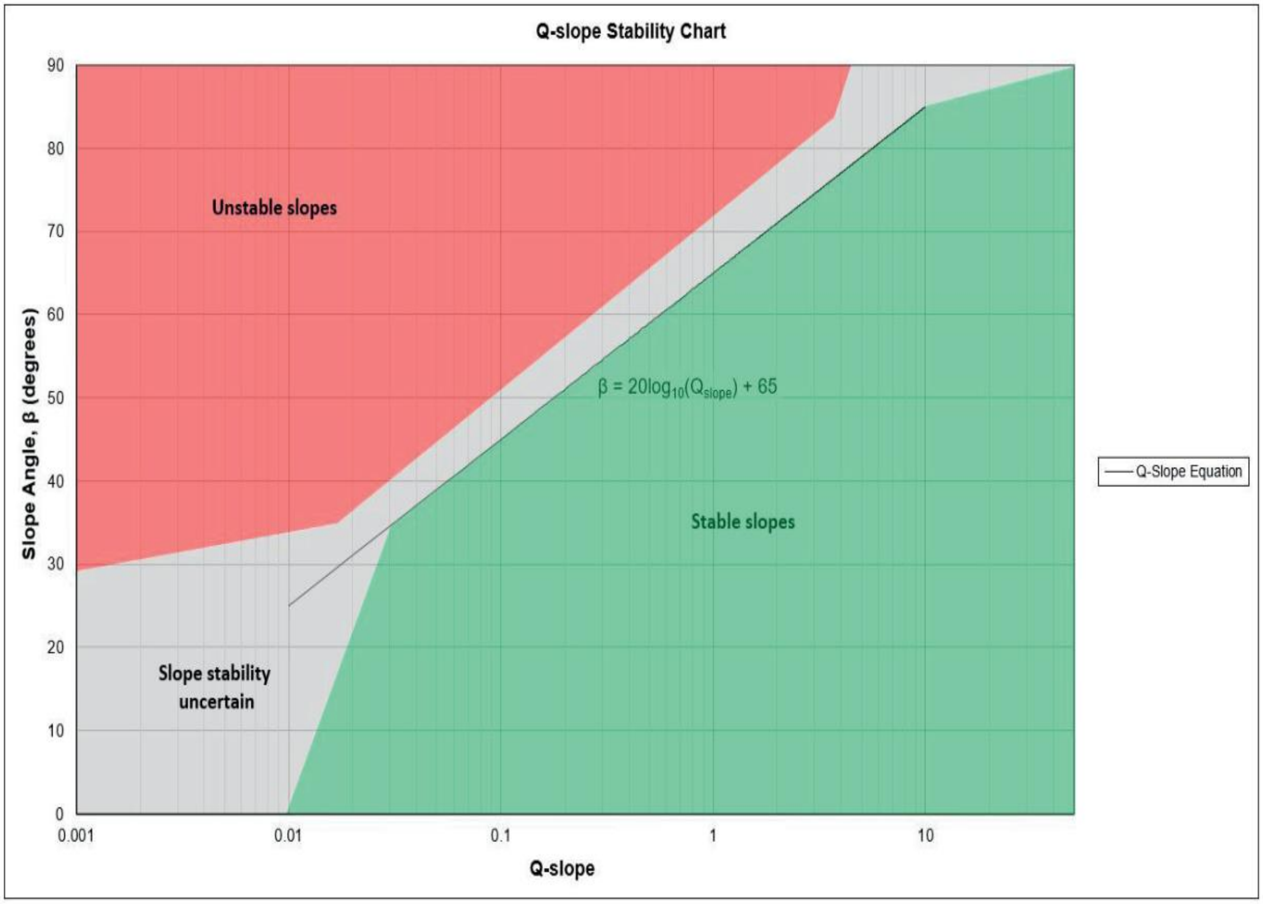

Fig 13: Q-slope Stability chart

5. Conclusion

This study provides some important information regarding the failure mechanism of the slope, the optimum overall slope angle and the optimum depth.

- The maximum stable slope angle modelled in the FLAC 2D is lower than the calculated slope angle through the Q-slope, and both these angles are considered to be stable as per the Q-slope stability chart and the FOS critical value.
- The optimum depth is estimated at 120 at Oroutumba pit 02 and 80m at Oroutumba pit 03.
- The models suggested that should the strain rate surpass the critical rate; the possibility of wedge failure could occur at Oroutumba pit 03 and planar failure at Oroutumba pit 02.

Author Contributions:

"Conceptualization, M.V.I. and V.M.; Methodology, M.V.I; Software, M.V.I.; Validation, M.V. I. and V.M.; Formal Analysis, M.V.I. and V.M.; Investigation, M.V.I; Resources, M.V.I and V.M.; Data Curation, V.M; Writing – Original Draft Preparation, M.V.I.; Writing – Review & Editing, V.M; Visualization, V.M; Supervision, V. M; Project Administration, V.M."

Acknowledgement

We would like to thank Ruforum, the Universities of Namibia and Zambia for their cooperation and for making this study possible through their capacity-building program. we would also to recognise the Dean, School of Mines, Dr. Bunda Besa for his valuable suggestions, encouragement, and guidance during the study.

Funding

There are no funding implications

Conflicts of Interest

The authors do not have any conflict of interest.

References

[1] P. N. Hooks, "SODALITE MINING PROJECT ENVIRONMENTAL IMPACT ASSESSMENT FOR MINING OF BLUE SODALITE DIMENSION STONE , RARE," no. April, 2021.

[2] (Ministry of Mines and Energy), "Dimension Stone in Namibia," 2022.

[3] Mindat, "Siderite from Sodalite mine, Orotumba (Oroutumba), Swartbooisdrif Dikes, Epupa, Kunene Region, Namibia," 2021. www.mindat.org/locentry-612446.html (accessed Aug. 31, 2023).

[4] "Kunene annual rainfall history," *Namibia Meteorological Service*. https://www.researchgate.net/figure/Total-annual-rainfall-recorded-at-Opuwo-town-Kunene-Region-from-1961-2019-Rainfall-data_fig1_344282253 (accessed Aug. 28, 2023).

[5] (Rough stone), "Sunset Sodalite from Namibia," 2023. www.roughstone.rocks/products/sodalite-from-namibia-1-pound (accessed Aug. 31, 2023).

[6] phillip collin, "Namibia Blue Sodalite - Blue Granite."

[7] Noetstaller Richard, "Historical Perspective and Key Issues," 1995.

[8] R. Leonard, M. Hauptfleisch, and R. Ellmies, "An Artisanal Mining Environmental Code of Practice for Namibia," *Min. Environ.*, no. 10, pp. 40–43, 2011.

[9] K. Gamage, A. Udara, and S. P. Chaminda, "A Review of Dimension Stone Extraction Methods," pp. 516–531, 2023.

[10] J. M. Nyambe and T. Amunkete, "Small-Scale Mining and Its Impact on Poverty in Namibia : A Case Study of Miners in the Erongo Region," *South. African Dev. Res. Netw.*, no. December, pp. 1–30, 2009, [Online]. Available: https://www.tips.org.za/research-archive/trade-and-industry/southern-african-development-research-network-sadrn/item/1930-small-scale-mining-and-its-impact-on-poverty-in-namibia-a-case-study-of-miners-in-the-erongo-region

[11] H. Crawford,A., Mooney,J., Musiyarira, "IGF Mining Policy Framework Assessment Namibia," no. September, p. 55, 2018.

[12] D. R. Gray *et al.*, "A Damara orogen perspective on the assembly of southwestern Gondwana," *Geol. Soc. Spec. Publ.*, vol. 294, pp. 257–278, 2008, doi: 10.1144/SP294.14.

[13] R. Rodeano, "Geological Behavior (GBR)," *Geol. Behav.*, vol. 2, no. 1, pp. 18–23, 2018, doi: 10.26480/gbr.02.2020.

[14] S. Jennings, P. Geo, R. C. Bell, and P. Geo, "Technical Report on Recent Exploration at the Kaoko Copper-Silver Property in Northwest Namibia for," 2010.

[15] H. E. E. C. Kazepua, "1091 EMP Mining claim 69356 at Oroutumba Village Swaartbooisdrift." Healthy Earth Enviromental Consultant, Windhoek.

[16] B. Goscombe, M. Hand, and D. Gray, "Structure of the Kaoko Belt, Namibia: Progressive evolution of a classic transpressional orogen," *J. Struct. Geol.*, vol. 25, no. 7, pp. 1049–1081, 2003, doi: 10.1016/S0191-8141(02)00150-5.

[17] I. Reliable, G. S. Index, G. Hoek-brown, T. G. Hoek-brown, and T. Mohr, "Rock mass properties," 1997.

[18] D. Studi and G. Seminar, *OPEN PIT SLOPE SLOPE DESIGN PERFORMANCE Slope Design in Weak Rocks*, no. August. 2015.

[19] N. Bar and N. Barton, "The Q-Slope Method for Rock Slope Engineering," *Rock Mech. Rock Eng.*, vol. 50, no. 12, pp. 3307–3322, 2017, doi: 10.1007/s00603-017-1305-0.

[20] R. Brummer, P. Andrieux, C. Detournay, and R. Hart, "FLAC and Numerical Modeling in Geomechanics 2003," *FLAC Numer. Model. Geomech. 2003*, 2003, doi: 10.1201/9781439833490.

[21] I. Itasca Consulting Group, "Flac 2D," 2023. https://www.itascacg.com/software/flac2d (accessed Jun. 01, 2023).

[22] Itasca Consulting Group Inc., "FLAC 8 Basics," p. 77, 2015.

[23] M. Cala, J. Flisiak, and A. Tajdus, "Slope stability analysis with FLAC in 2D and 3D," pp. 50–53.

[24] Y. Zheng, L. Zheng, H. Zhan, Q. Huang, C. Jia, and Z. Li, "Study on Failure Mechanism of Soil – Rock Slope with FDM-DEM Method," 2022.

[25] M. Zhu, C. Ma, and R. Tang, "Slope Stability Analysis of Open Pit Mine Based on Finite Difference Method," pp. 208–211, 2009, doi: 10.1109/ICIC.2009.258.

[26] D. W. Fleck, "WSDOT Geotechnical Design Manual M 46-03.08. Chapter 7: Slope Stability Analysis," no. October, pp. 522–624, 2013.

[27] M. Duncan, Wyllie;Christopher, *Rock slope engineering (civil and mining)*, 4th ed., vol. 5, no. 3. Newyork: Taylor & Francis e-Library, 2005.

[28] T. G. Sitharam and A. Hegde, "Stability analysis of rock-fill tailing dam : an Indian case study Stability analysis of rock-fill tailing dam : an Indian case study," vol. 6362, no. August, 2016, doi: 10.1080/19386362.2016.1221574.

[29] A. B. Khalkhali and M. K. Koochaksaraei, "Computational Engineering and Physical Modeling Evaluation of Limit Equilibrium and Finite Element Methods in Slope Stability Analysis-Case Study of Zaremroud Landslide, Iran," *Comput. Eng. Phys. Model.*, vol. 2, no. 3, pp. 1–15, 2019, [Online]. Available: http://creativecommons.org/licenses/by/4.0/

[30] H. Wang, Z. Chen, and D. Zhang, "Rock slope stability analysis based on FLAC 3D numerical simulation," vol. 173, pp. 375–379, 2012, doi: 10.4028/www.scientific.net/AMM.170-173.375.

[31] . K. S., "Stability Analysis of Open Pit Slope By Finite Difference Method," *Int. J. Res. Eng. Technol.*, vol. 03, no. 05, pp. 326–334, 2014, doi: 10.15623/ijret.2014.0305062.

[32] M. ATAEI and S. BODAGHABADI, "Comprehensive analysis of slope stability and determination of stable slopes in the Chador-Malu iron ore mine using numerical and limit equilibrium methods," *J. China Univ. Min. Technol.*, vol. 18, no. 4, pp. 488–493, 2008, doi: 10.1016/S1006-1266(08)60281-3.

[33] J. read;peter Stacey, *Guideline for open pit slope design*, vol. 56, no. 2. South Africa: Csiro, 2010. doi: 10.1016/0002-9416(69)90237-1.

[34] B. Azarfar, S. Ahmadvand, J. Sattarvand, and B. Abbasi, "Stability Analysis of Rock Structure in Large Slopes and Open-Pit Mine: Numerical and Experimental Fault Modeling," *Rock Mech. Rock Eng.*, vol. 52, no. 12, pp. 4889–4905, 2019, doi: 10.1007/s00603-019-01915-4.

[35] E. Hoek and E. T. Brown, "The Hoek–Brown failure criterion and GSI – 2018 edition," *J. Rock Mech. Geotech. Eng.*, vol. 11, no. 3, pp. 445–463, 2019, doi: 10.1016/j.jrmge.2018.08.001.